https://doi.org/10.1016/j.apenergy.2023.121554

Wind Farm Layout and Hub Height Optimization with a Novel Wake Model

Haiying Sun[a*], Hongxing Yang[b**]

[a]School of Marine Science and Engineering, South China University of Technology, Guangzhou, China
[b]Renewable Energy Research Group, Department of Building Environment and Energy Engineering, The Hong Kong Polytechnic University, Hong Kong

Abstract

This paper comprehensively investigates the impact of wind turbine layout and hub height on power generation of wind farm. Firstly, an engineering three-dimensional (3-D) wind turbine wake model is improved by the artificial neural network (ANN) technology. The novel 3-D ANN wake model reaches more than 99% accuracy of the original wake model. It can save about 80% of the computational time when predicting the downstream wind speed. Secondly, the influence of wind turbine hub height and position on the equivalent wind speed (EWS) and power is deeply studied. Specially, when reducing the hub height of the downstream wind turbine, both the wake impact from upstream turbines and EWS will decrease, so the overall influence should be assessed according to the specific situation. Finally, the problem of wind farm layout and height optimization is investigated. According to this study, simultaneously optimizing these two factors can obtain a better result than optimizing each factor individually. If economic factor is additionally considered, the optimized hub height and power output results will be quite different. Therefore, considering more factors is important to obtain an appropriate wind farm layout.

Keywords: Wake effect; Artificial neural network; Hub height; Wind farm layout optimization.

1. Introduction

Energy demand is a significant factor for socio-economic development, which increases with the global population and economy growth annually [1]. Renewable energy is an ideal energy source to solve the serious problems related to global warming, pollution, and energy shortage. At present, wind power is one of the most promising energy resources because of its inexhaustible and clean characteristics. Hybrid models have been proposed to improve the accuracy of wind speed forecasting [2]. To improve the power generation of wind farms, the wind farm optimization method has been widely investigated and applied. Various parameters can be optimized, such as the type of wind turbine, layout, cable, etc. The hub height optimization has prominent influence on the power generation of wind farm, which therefore

* Corresponding author. *E-mail address:* sunhaiying@scut.edu.cn; haiying.sun@connect.polyu.hk
** Corresponding author. *E-mail address:* hong-xing.yang@polyu.edu.hk

attracts increasing attention.

Alam, et al. [3] reviewed a series of wind turbines and studied the relationship between energy production and hub height. They optimized hub height to maximize the energy production in Saudi Arabian wind conditions. Albadi and El-Saadany [4] studied how to match wind turbine sites by considering wind speed characteristics, power curve parameters, turbine size, and tower height. It has been found that higher tower is not always the most desirable and there is an optimal tower height for each turbine. Chen, et al. [5] developed a method to investigate the optimal hub height. Through the research, it was confirmed again that higher hub height is not always ideal for the entire wind farm [6]. Compared to the layout with an identical hub height, those with multiple hub heights can increase the energy output and reduce the unit power cost. This phenomenon is profound in complex-terrain wind farms [7]. Chen, et al. [8] investigated the impact of hub height on the power generation of a small wind farm. It was concluded that with a fixed number of turbines, the layout with different hub heights can increase the power, but the cost per unit power may also increase. Lee, et al. [9] presented a hub height optimization method, aiming at improving the annual net profit. The conclusion is that the optimal hub height increases with the average wind speed and wind shear exponent. The rated and cut-out wind speeds can seriously affect the optimized hub height. MirHassani and Yarahmadi [10] also studied the effect of hub height on the total power. A mathematical algorithm was introduced to simulate the wake decay of Jensen model in terms of interaction matrix. Abdulrahman and Wood [11] optimized the layout of wind farm by selecting turbines and changing hub heights. They pointed out that applying various turbines and hub heights can achieve a better trade-off between power and cost. Vasel-Be-Hagh and Archer [12] analyzed how the hub height optimization influences the power generation of wind farm. Results from Large-Eddy Simulations (LES) showed that hub height optimization was beneficial, with the net gain higher than that calculated by the linear model. Biswas, et al. [13] proposed a multi-objective evolutionary algorithm to obtain optimal windfarm layouts. Song, et al. [14] optimized a flat-terrain wind farm with multiple hub heights. All positions and hub heights have been optimized simultaneously. From these studies, the 3-D optimization has better solutions than the 2-D optimization in improving power generation. The summary of studies related to hub height optimization is demonstrated in Table 1. So far, the research on optimizing wind turbine hub height is still limited. Among most of these studies, only a few representative hub heights were considered, therefore the actual best results could not be obtained.

Table 1 Summary of wind turbine hub height optimization.

Scholar	Year	Optimal hub height design	Wake model
Albadi and El-Saadany [4]	2010	Hight range: 30 m to 160 m	N.A.
Chen, et al. [5]	2013	Hight range: 40 m to 140 m	Extension of Jensen wake model
Chen, et al. [6]	2013	Hight range: 40 m to 600 m	Extension of Jensen wake model
Chen, et al. [8]	2013	Two hub heights: 50 m and 78 m	Extension of Jensen wake model
Lee, et al. [9]	2015	Hight range: 30 m to 300 m	N.A.
Chen, et al. [7]	2016	Two hub heights: 50 m and 78 m	Extension of Jensen wake model
MirHassani and Yarahmadi [10]	2017	Two hub heights: 50 m and 78 m	Extension of Jensen wake model
Abdulrahman and Wood [11]	2017	Hight range: 80 m to 140 m	Extension of Jensen wake model
Vasel-Be-Hagh and Archer [12]	2017	Two hub heights: 57.5 m and 100 m	Extension of Jensen wake model
Biswas, et al. [13]	2017	Three hub heights: 60 m, 67m and 78 m	Extension of Jensen wake model
Song, et al. [14]	2018	Hight range: 46 m to 780 m (interval at 2 m)	Extension of Jensen wake model

On the other hand, the wake effect is even more important and complex in hub height optimization. A common method to solve the wake problem is adopting an extension of Jensen wake model. However, the vertical wind speed distribution cannot be considered with a such simplified model. Sun and Yang [15] derived a 3-D wake model that considers the wind speed variation in the vertical direction. Dou, et al. [16] proposed a 3-D yawed wake model to optimize the yaw angle misalignment. Gao, et al. [17] derived a 3-D elliptical wake model and validated it with wind-field experiments. To improve the calculation performance of 3-D wake models, machine learning methods have been applied to the wake estimation. Ti, et al. [18] employed artificial neural network (ANN) and computational fluid dynamics (CFD) to develop a 3-D model to simulate wake effect. Then, the wake model was applied to improve the power prediction of wind farm [19]. Luo, et al. [20] developed a learning-based wake model based on the CFD simulation method to optimize the wind farm layout. With 3-D wake models, more problems can be investigated in-depth. Zhen, et al. [21] developed a surrogate 3-D wake model to optimize wind farm layout and proved that different hub heights in a wind farm can substantially reduce the wake effect. Although ANN method can reduce the calculation cost, the related 3-D wake models are based on CFD methods, of which the computational time is still too high to solve the wind farm layout optimization problem.

To cope with the aforementioned research gaps, this study proposes a fast and accurate 3-

D ANN wake model. The new model is based on the original 3-D wake model, which can describe the wind speed at any spatial position. Therefore, it takes advantages of the high accuracy of the original wake model and the fast computation of ANN technology. For a specific wind turbine, the measured data will be used to develop the wake model and the ANN model can be further obtained by training the wake model. By using the 3-D ANN wake model, the wind farm layout and hub height optimization problems are further investigated. The rest of this paper is structured as follows. Section 2 introduces a 3-D wind turbine wake model and trains it to a new 3-D ANN wake model. Section 3 reveals the impact of hub height on power output of single and two wind turbines. Section 4 analyzes the hub height optimization problem and the optimized results. Section 5 summarizes the main conclusions. The output of this paper is meaningful to the development of the wind energy industry. With the newly-proposed 3-D ANN wake model, the layout and hub heights of wind turbines can be simultaneously optimized to improve the power generation of the entire wind farm.

2. Development of the 3-D ANN wake model

2.1 The engineering 3-D wake model

A practical engineering wind turbine wake model is applied in this study. By using this model, wind speed and deficit at any spatial position could be calculated accurately. Compared with traditional 1-D and 2-D wind turbine wake models, this 3-D model is more reasonable, which makes it possible to investigate complicated problems, such as hub height and layout optimization on complex terrain [15]. The illustration of wind speed from the wake model is demonstrated in Figure 1.

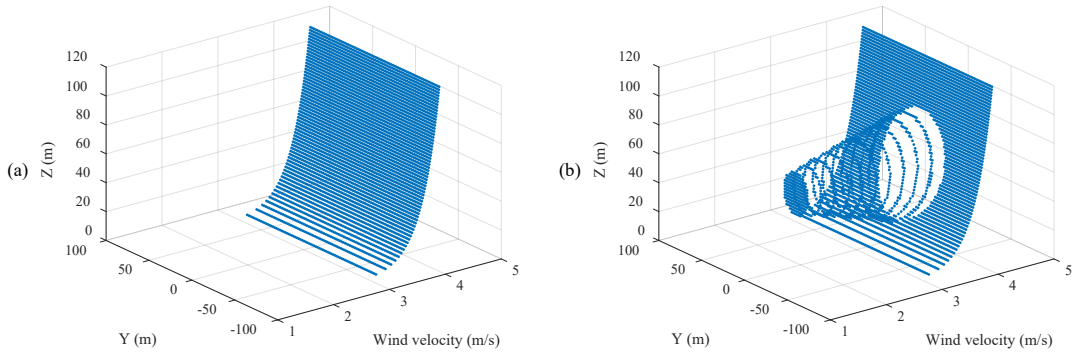

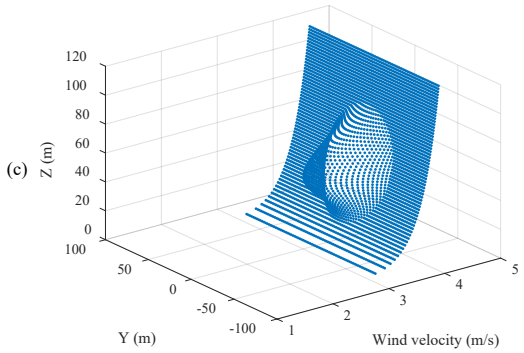

Figure 1 Schematic of the 3-D wake model at different downstream positions: (a) incoming wind distribution; (b) wind distribution behind a wind turbine; and (c) wind distribution at a far-wake position.

The wake model has three assumptions. Firstly, the distribution of wind speed deficit in any downwind vertical plane is Gaussian-distributed. The second assumption is related to the momentum conservation theory [22]. To be specific, the total flow flux at any downstream distance is the same. Since the incoming wind condition is constant, a circular area with the wake effect radius is applied to consider the downstream wake. The circular area is right behind the turbine, and its total flow flux should be the same at any downstream position. The last assumption states that the wind speed is continuous on the wake boundary.

Assuming U_0 is the incoming wind speed, U is the actual downstream wind speed. According to reference [15], U can be described by equation (1):

$$U = A\left(\frac{1}{2\pi\sigma^2} e^{-\frac{y^2+(z-h_0)^2}{2\sigma^2}}\right) + B + U_0 \tag{1}$$

where h_0 is wind turbine's hub height. r_w is the radius of wake-affected area, which varies in the downstream direction. σ is defined as r_w divided by the parameter C, which is determined according to the actual operating condition. Q represents the total flow flux of the wake-affected circular area with a radius of r_w. Finally, A and B are two parameters [15] calculated by equation (2).

$$\begin{cases} A = \dfrac{Q - \int_{h_0-r_w}^{h_0+r_w} 2\sqrt{r_w^2 - (z-h_0)^2}\, U_0 dz}{\left(1 - e^{-\frac{C^2}{2}} - \frac{C^2}{2} e^{-\frac{C^2}{2}}\right)} \\ B = -\dfrac{AC^2}{2\pi r_w^2} \cdot e^{-\frac{C^2}{2}} \end{cases} \tag{2}$$

By comparing with the data of wind tunnel experiments from references [23] and [24], the 3-D wake model has proven to be accurate in calculating the single turbine wind speed deficit.

Furthermore, Sum of Squares [25] is adopted to account wind deficits in the overlap space affected by several wind turbines [26]. If the i^{th} wind turbine is influenced by other n wind turbines' wakes, equation (3) should be adopted.

$$U_i = U_0 - \sqrt{\sum_{j=1}^{n}[A_j(\frac{1}{2\pi\sigma_j^2}e^{-\frac{(y-y_j)^2+(z-h_0)^2}{2\sigma_j^2}})+B_j]^2} \tag{3}$$

The 3-D wake models are useful when designing hub heights and optimizing the layout of nonuniform wind farm with different wind turbines. However, the application of wake model still has limitations because of the high computational cost. In 3-D wake models, the wind speed cannot be calculated independently, and all other parameters should be calculated first. Therefore, the computation time of layout optimization will be even longer when applying these wake models.

To solve the aforementioned problems, ANN method is integrated with the 3-D wake model in order to improve its calculation performance. The newly proposed 3-D ANN wake model is trained by data from the original wake model. The model can calculate the wind speed at each position independently, and save the computation time significantly. Thus, the 3-D ANN wake model can calculate wind speeds accurately and quickly.

2.2 Development of the 3-D ANN wake model

Several measurements were organized in Shiren wind field that locates in northern China (41˚N, 114˚E) [27]. The target wind turbine's rotor diameter is 77 m and the hub height is 65 m [28]. The constant wind is considered in this study, and Figure 2 demonstrates the profile of the incoming wind speed. The wind speed at the hub height is 12.7 m/s.

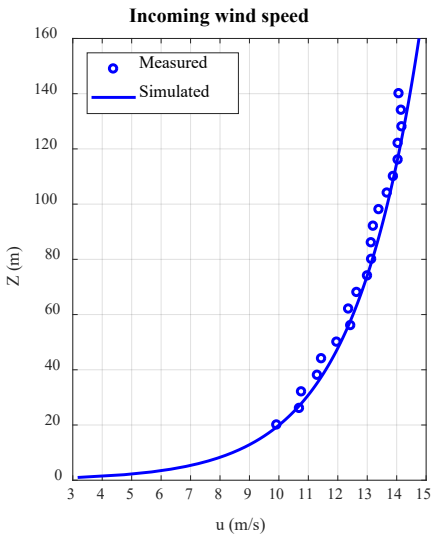

Figure 2 Incoming wind speed

In this paper, the profile of inflow is simulated by the log law [29], as expressed in equation (4).

$$U_0 = \frac{U^*}{k}\ln\left(\frac{z}{z_0}\right) \tag{4}$$

where U^* represents the friction velocity. z_0 is the surface roughness length. k is the Von Kármán constant. The original 3-D wake model has been validated and calibrated by the measurements at several downstream distances [30]. The power performance of the wind turbine is also measured from the wind farm. Then, the model can be applied to predict wind deficits with higher resolutions at more downstream distances. In this study, the high-resolution results are used to train an accurate 3-D ANN wake model. The resolutions in Y direction, Z direction, and the downstream direction are 0.01D, 0.01D and 1D, respectively (D is the rotor diameter). The process of the model development is demonstrated as follows.

Step 1: Data collection and preprocessing. The original data should be collected from the original 3-D wake model for the development of the ANN model. Then, the dataset should be normalized for the ANN model development.

Step 2: Model establishment. The basic structure of the 3-D ANN wake model consists of input layer, hidden layer(s), and output layer. The input layer contains coordinates of positions. The output layer contains wind deficits. The numbers of layers and neurons in each hidden layer should be determined according to the evaluation results.

Step 3: Model training. The effective dataset will be divided into a training set, a validation set, and a test set. The model should be trained by the training set. The validation set are used to evaluate the effectiveness of the model in each training epoch. The numbers of layers and neurons should be adjusted accordingly.

Step 4: Model testing. After the training process, the performance of the ANN model should be tested by the test dataset. The mean square error (MSE) value is applied to evaluate the predicted results.

After these four steps, the well-trained structure of 3-D ANN wake model is demonstrated in Figure 3. It has one input layer, one output layer, and two hidden layers. To be specific, the input layer has three neurons, which are the three coordinates in spatial positions. Two hidden layers have five and six neurons, respectively. The output layer has one neuron, which is the wind deficit at the corresponding position denoted in the input layer.

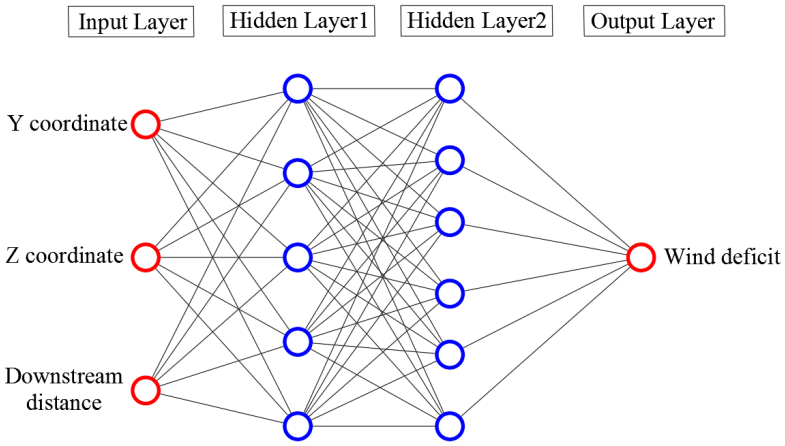

Figure 3 Structure of the 3-D ANN wake model.

Sigmoid function is used in hidden layers. The maximum training epoch is set as 1000. The training goal is to make the MSE lower than the reference value, of which MSE is computed as Equation (5).

$$\mathrm{MSE} = \frac{1}{n}\sum_{i=1}^{n}\left(Y_i - \hat{Y}_i\right)^2 \tag{5}$$

n is the number of data points on all variables, and Y_i is the vector of observed values of the variable being predicted, with $\hat{Y}_i$ being the predicted values.

In this study, the target value of MSE is set as 10^{-6}, which means the training goal will be achieved when MSE is lower than 10^{-6}. Data are separated into a training set, a validation set and a test set, which are 70%, 15% and 15% of all data, respectively. The evolution of validation progress is shown in Figure 4. The time to train this model is 831 seconds.

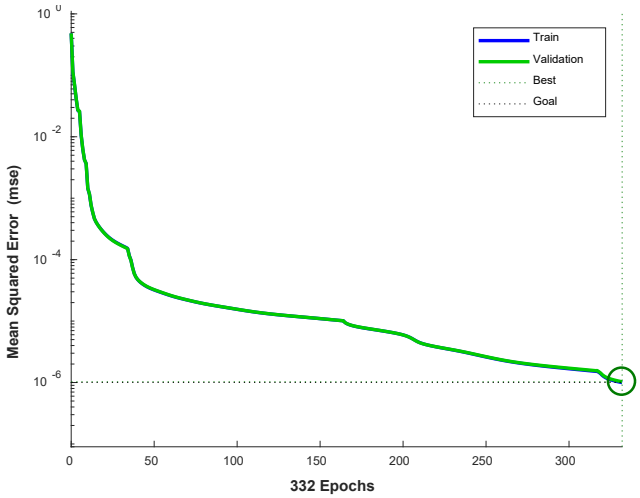

Figure 4 Validation progress of the 3-D ANN wake model.

MSEs of both training and validation progresses drop quickly in the beginning 50 steps, and then decrease slowly. The training process stops at the 332nd epoch, when the criterion is

met. Figure 5 demonstrates the wake model's accuracy performance.

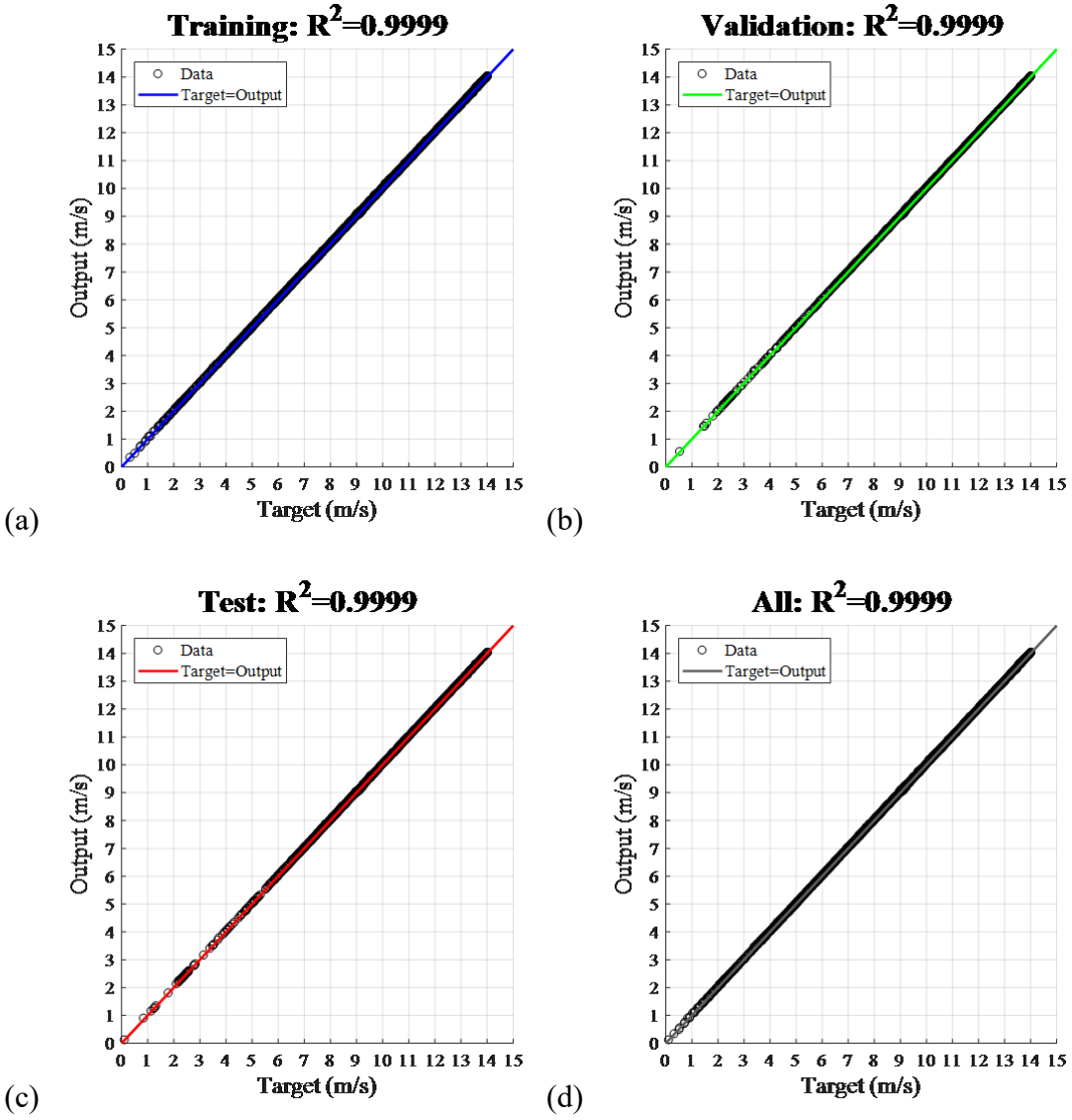

Figure 5 Accuracy performance for: (a) Training data; (b) Validation data; (c) Test data; and (d) All data.

Coefficient of determination is adopted to evaluate the model's performance, which is denoted by R^2. From Figure 5, all values of R^2 are larger than 0.9999 in all datasets, indicating the structural effectiveness and the high accuracy of the trained model. Therefore, the wind deficit can be accurately calculated by this 3-D ANN wake model.

2.3 Feasibility of the 3-D ANN wake model

One advantage of the new 3-D ANN wake model is that it could predict the wind deficit at any position independently. Since there is no need to calculate other parameters, such as total flow flux, huge computational time can be saved. The 3-D ANN wake model is programed in MATLAB software, and the performance of the model is tested using a computer with an Intel

Core i7-6700 CPU, 4 cores and 16 GB RAM. Computing 100 wind farm layouts at a time, each with 30 wind turbines, it takes 36.4 and 196.2 seconds to calculate the wake effect with 3-D ANN wake model and the original wake model, respectively. Including the model training time, the total computing time is saved by about 80%.

Another advantage of the model is the high accuracy, which makes it possible to evaluate wind turbine's power generation under wake effect. With the characteristics of high accuracy and low computation cost, the 3-D ANN wake model could be further applied to solve other complicated problems, including optimizing wind turbine hub height and wind farm layout in complex terrains.

The 3-D ANN wake model also has limitations. Like other ANN models, this model is only applicable to the specific working conditions. If users want to calculate other wind turbines, the model should be trained for the new working conditions. Another thing to note is that plenty of data should be obtained in advance to train the model. In this study, the data come from the 3-D wake model validated previously. In other cases, the CFD simulation and experimental data could also be used, as long as the dataset is large enough. The large amount of data is a necessary condition for the high accuracy of the model. For wind farms with complex wake conditions, the overfitting risk should be considered. Parameters or techniques should be included to limit and constrain how much wake detail the model learns.

3. Impact of hub height

In this section, the 3-D ANN wake model is first trained by data measured of an operating wind turbine in Hebei Province [17]. The rated power is 1513 kW, the cut-in and cut-out wind speeds are 3m/s and 25 m/s, respectively. The specifications of the experimental wind turbine type are listed in Table 2.

Table 2 Specifications of the wind turbine.

Parameter	Value
Rated power (kW)	1513
Hub height (m)	65
Rotor Diameter (m)	77
Cut-in wind speed (m/s)	3.0
Rated wind speed (m/s)	11.0
Cut-out wind speed (m/s)	25.0
Rotate speed (rpm)	9.7 - 19.5
Rated frequency (Hz)	50

The power curve is demonstrated in Figure 6, where red circles represent the data from the operating turbine, and the black line is the simulated result from the 3-D ANN wake model.

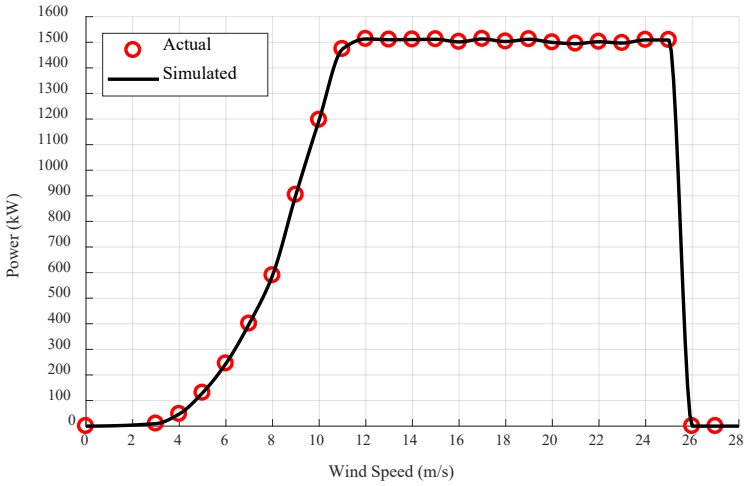

Figure 6 Power performance of the experimental wind turbine.

3.1 Single wind turbine

For one wind turbine, increasing its hub height will generally increase the power performance to some extent. Because of the ground roughness, the incoming wind always increase with height, as demonstrated in Figure 2. When hub height increases, the equivalent wind speed (EWS) will increase accordingly. Figure 7 demonstrates the impact of hub height on EWS. Obviously, EWS increases with hub height, but the increase will not always lead to the improvement of power generation. Figure 8 demonstrates the relationship between power output and hub height. When EWS is greater than the rated wind speed, the power of wind turbine will remain as the rated power. Even with a light change in hub height, the power remains the same and is not sensitive to the change of EWS. When the hub height decreases a lot and EWS is less than the rated wind speed, the power will decrease as well.

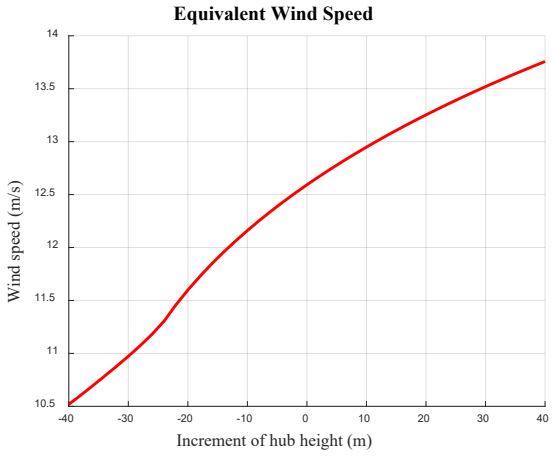

Figure 7 Impact of hub height on EWS.

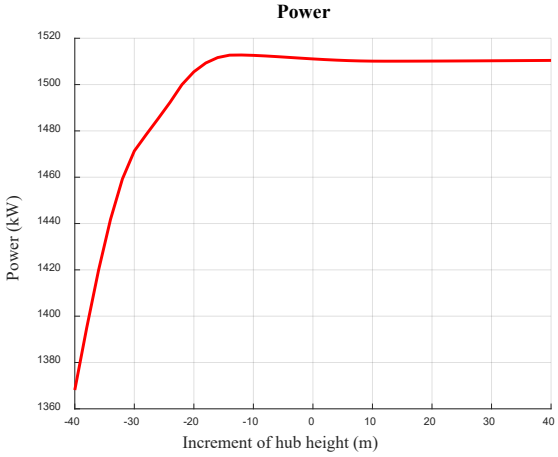

Figure 8 Impact of hub height on power output.

3.2 Two wind turbines - Changing the downstream distance

Due to the wake effect, changing hub height will not only affect the wind turbine itself, but also other nearby wind turbines. Therefore, it is necessary to investigate how wind turbines influence each other. In the following part, the two adjacent wind turbines will be taken as an example to investigate how a wind turbine influences another one when its position and hub height change.

Changing the downstream distance between two wind turbines has no influence on the upstream wind turbine. However, increasing downstream distance will improve downwind turbine's power performance. Figure 9 and Figure 10 show the impact of downstream distance on the EWS and power of the downstream turbine at different hub heights.

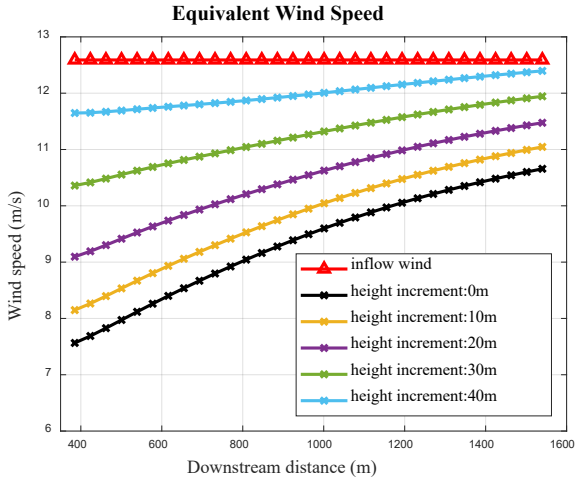

Figure 9 Impact of downstream distance on downstream wind turbine's equivalent wind speed.

EWS of the downstream turbine is much smaller than that of the upstream turbine. At the original height, turbine's EWS increases from 7.6 m/s at 385 m downstream position to 10.7 m/s at 1540 m downstream position. Increasing the hub height will also increase the EWS

significantly. At 385 m downstream position, when the hub height increases by 40 m, EWS increases to 11.7 m/s. At 1540 m downstream position, even if with a height increment of 40 m, EWS does not return to the incoming wind speed. Therefore, EWS is sensitive both to hub height and downstream distance.

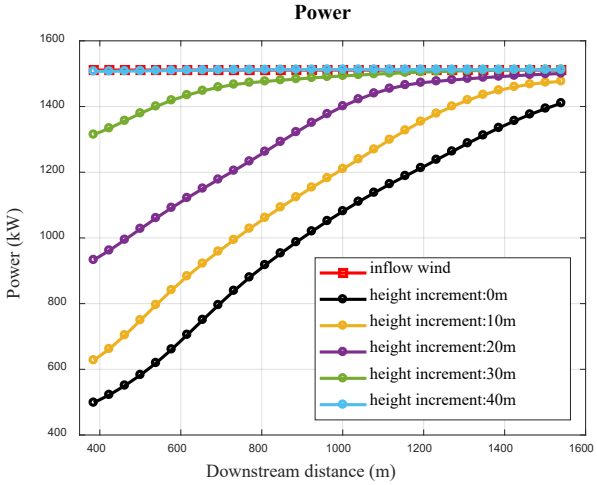

Figure 10 Impact of downstream distance on downstream wind turbine's power.

The effect of downstream distance on power is similar to the effect on EWS. At a certain height, increasing downstream distance will improve downstream turbine's power to some extent. However, as EWS increases to the range of rated and cut-out wind speeds, the power performance will not continue improving. With a height increment of 10 m, the power at the 385 m downstream position increases to the 1540 m downstream position. Here the power output has not reached the rated power yet. As the height increases by 20 m, the power increases from 940 kW at the 385 m downstream position to the rated power at around 1400 m downstream position, and then remains at this power. If the hub height further increases, less downstream distance is required to reach the rated power. Actually, when the height increases by 40 m, the power reaches the rated power from the downstream position of 385 m, and will not further increase in the downstream direction.

Increasing downstream distance is a useful way to improve EWS of the downstream turbine. However, it is not always effective in improving power. If the EWS is greater than the rated wind speed, the power does not continue increasing. With a larger hub height, the downwind turbine can reach the rated power at a relatively close downstream position. Therefore, with the 3-D wake model, increasing the downstream distance and the hub height are two effective methods to improve downwind wind turbines' power generation.

3.3 Two wind turbines - Changing the cross-wind horizontal distance

Changing the cross-wind horizontal distance is another way to improve downstream wind turbine's power performance. Figure 11 and Figure 12 show the impact of cross-wind horizontal

distance on downstream wind turbine's power output at various hub heights.

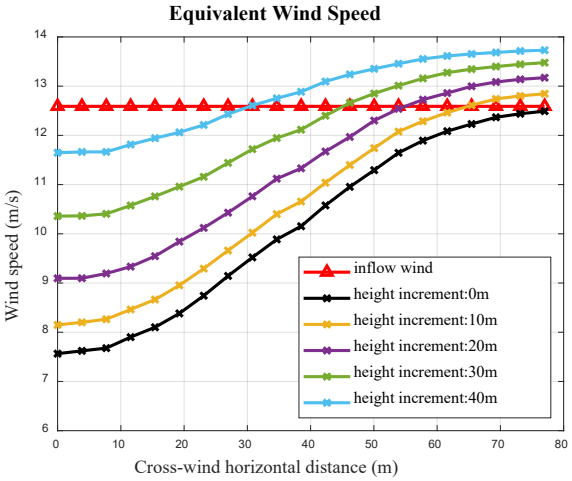

Figure 11 Impact of cross-wind horizontal distance on downstream wind turbine's equivalent wind speed (5D downstream position).

As demonstrated, when a wind turbine is influenced by wakes, increasing the cross-wind horizontal distance will avoid the serious wake effect and lead to an increase in the EWS. For the original hub height, the EWS increases from 7.6 m/s at the wake centerline to 12.5 m/s at the position of 77 m cross-wind horizontal distance. For a higher hub height, the turbine can have a larger EWS at the same position. When hub height increases to 40 m, it only needs to move 40 m horizontally to avoid the wake influence. If the cross-wind horizontal distance further enlarges to 77 m, the EWS will reach 13.7 m/s.

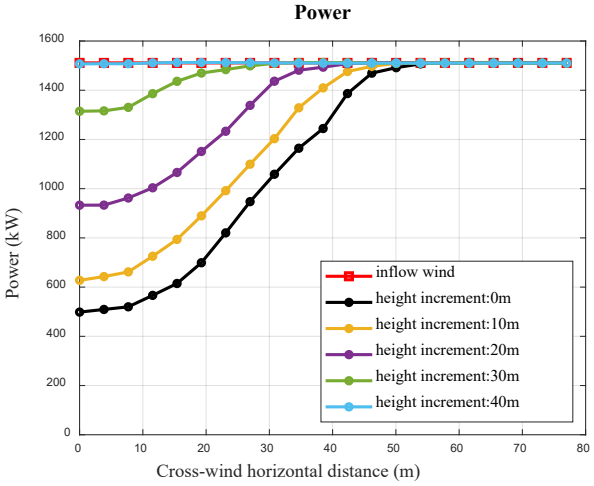

Figure 12 Impact of cross-wind horizontal distance on downstream wind turbine's power (5D downstream position).

The cross-wind horizontal distance also has significant influence on downwind wind turbine's power output. At low positions, increasing the cross-wind horizontal distance can significantly increase the power output. For example, at the original hub height, the power at

the central position is only 500 kW, then with the cross-wind horizontal distance increases to 55 m, it quickly increases to the rated power of 1513 kW. While when the hub height is larger than 40 m, the power output performance will not continue improving. This height maybe different in other cases.

3.4 Two wind turbines - Changing the hub heights

Changing hub heights of either upstream or downstream wind turbines may help to improve both wind turbines' power generation. For the case that has a single turbine, the EWS can be improved by increasing the hub height. However, for two or more wind turbines, each wind turbine's EWS can be improved through both increasing and decreasing the hub height.

3.4.1 Changing the upstream wind turbine

Changing upwind turbine's hub height will have significant impact on both itself and the downstream one. Actually, the impact on itself is the impact on a single wind turbine, which has been studied in Section 3.1. This section only discusses the impact on downstream wind turbine.

Figure 13 and Figure 15 show the impact of the upwind turbine's hub height on the downwind turbine's EWS and power output. From results, downwind turbine has the smallest EWS when fixed at the same height with the upstream one. The wind deficit is the maximum at the hub height. Therefore, no matter increasing or decreasing the upstream hub height, the wake impact on the downstream turbine will be weakened. This phenomenon is especially noticeable when two wind turbines are close. When wind turbines' interval is 5D and the hub heights are the same, the EWS of the downwind turbine is only 8.7 m/s. If the upstream one increases or decreases the hub height by 40 m, the wind speed can increase to 10.4 m/s. When the distance is 10D, the increment of the EWS under the same changing condition will be 1.9 m/s (from 8.7 m/s to 10.6 m/s).

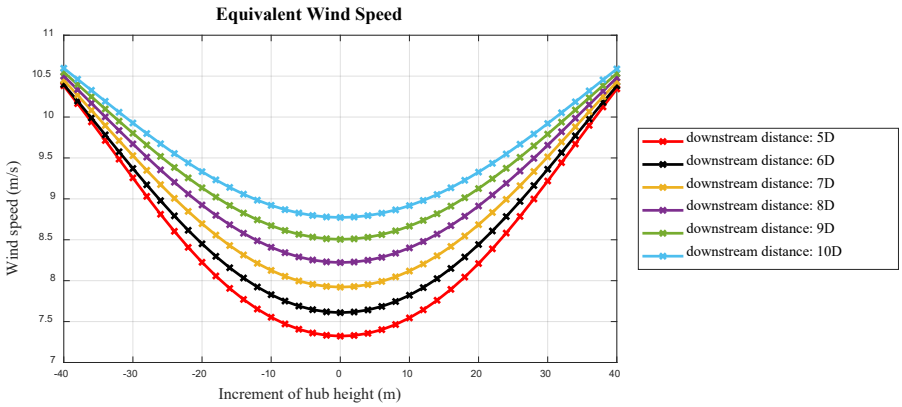

Figure 13 Impact of upstream wind turbine's hub height on downstream wind turbine's equivalent wind speed.

The impact of upstream turbine's hub height on downstream one's power is even more pronounced. At the 5D downstream position, the power could be improved from 450 kW to 1330 kW. While at the 10D downstream position, the power output can be improved from 830 kW to 1400 kW. One thing to note is that changing a certain height may have different impacts on power output. At all downstream distances, the power increments caused by the hub height increment from 30 m to 40 m are much larger than those from 0 m to 10 m.

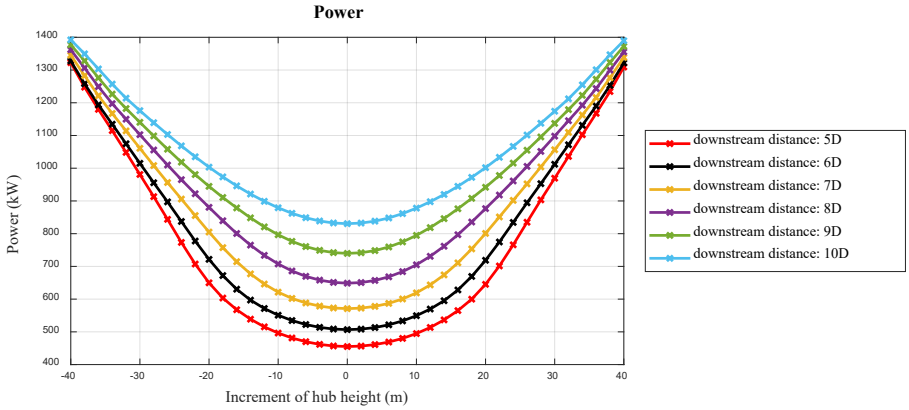

Figure 14 Impact of upstream wind turbine's hub height on downstream wind turbine's power output.

3.4.2 Changing the downstream wind turbine

Changing downstream turbine's hub height has almost no influence on the upstream one. However, the influence on itself is much more complicated.

Figure 15 and Figure 16 demonstrate the impact of downstream wind turbine's hub height on its EWS and power output. When increasing hub height, EWSs and power outputs at all downstream positions increase significantly. On the one hand, the incoming wind is larger at a higher position. On the other hand, increasing downstream wind turbine's hub height can avoid the wake impact from the upstream one. Correspondingly, the power also increases with the EWS.

When decreasing the hub height, where the increment of hub height is smaller than zero, the EWS will not change with the hub height monotonically. At the 10D downwind position, the EWS decreases with the hub height increasing. At the 9D downstream position, this trend is not very clear. Especially when the hub height decreases by 20 m, the EWS maintains at 8.2 m/s and it does not further decrease with hub height. While for positions in front of 8D, the relationship between hub height increment and EWS is curvilinear. At the 5D downstream position, this phenomenon is most significant. When the hub height first decreases from 0 m to -10 m, the EWS decreases from 7.3 m/s to 7.1 m/s. Then EWS has a reverse trend below the -10 m height, which increases from 7.1 m/s to 7.9 m/s as hub height decreases from -10 m to -40 m. The power change follows this trend, first decreasing from 450 kW to 410 kW and then gradually increasing to 580 kW.

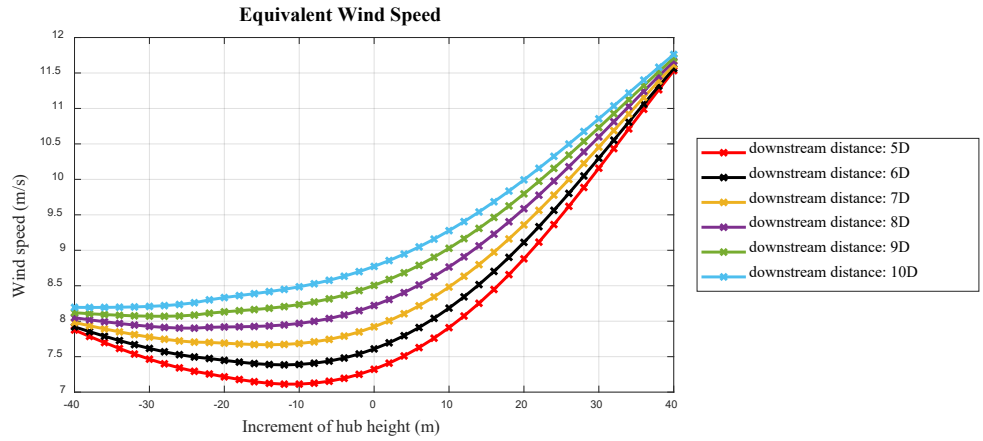

Figure 15 Impact of downstream wind turbine's hub height on its equivalent wind speed.

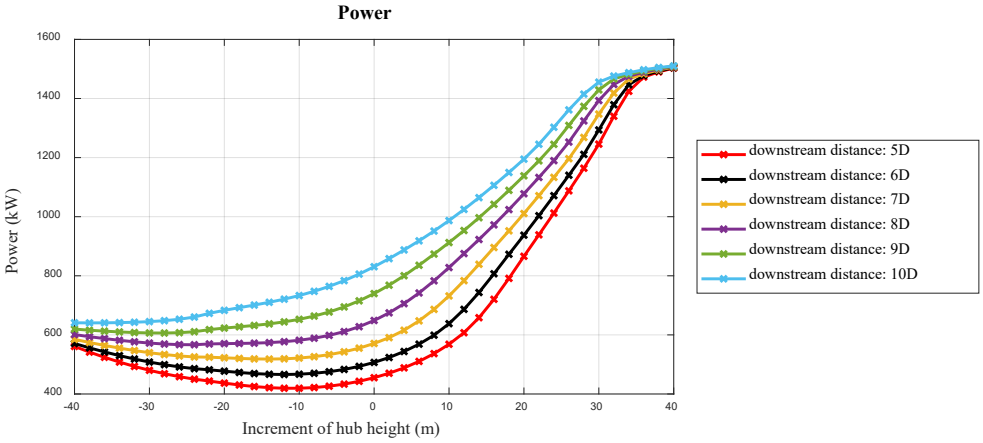

Figure 16 Impact of downstream wind turbine's hub height on its power output.

Changing a wind turbine's hub height has complicated influence on its wind farm. Because it will not only affect the wind turbine itself, but also other nearby wind turbines. For a single wind turbine, its EWS will change with the hub height monotonically. Increasing hub height will achieve a larger EWS, while decreasing the hub height will result in a smaller EWS. The specific increment is connected to incoming wind's profile. For the situation of two turbines, changing hub height of a turbine has a very different effect on itself and the other wind turbine. Increasing the upstream hub height will decrease the wake impact on the downwind one, which will increase EWSs of both upwind and downwind turbines. Increasing the downstream hub height has no impact on the upwind one but can increase the EWS of the downwind turbine. Decreasing the upstream hub height will reduce the EWS of the upwind turbine, but this may also reduce the wake's impact on the downwind turbine and increase the EWS. Decreasing downwind turbine's hub height has no impact on the upstream wind turbine, but it may have different impact on itself. The EWSs of downstream wind turbines may increase or decrease, which depends on the interval between turbines.

Generally, the power output of a wind turbine corresponds to its EWS. However, duo to

the power curve, a higher EWS will not always lead to a higher power output. When EWS is in the range of cut-in and rated wind speeds, the power will increase with EWS increases. While when EWS is larger than the rated wind speed, turbine's power will maintain at the rated power. Therefore, the influence of hub height on the power performance should be considered from aspects of both EWS and power curve.

4. Wind turbine hub height and layout optimization

Since optimizing wind farm's hub heights and layout can improve the power generation, this section will discuss the influence of these two strategies.

4.1 Optimization method

Genetic Algorithm (GA) is widely used to optimized the wind farm layout because of its high-efficiency advantage [31]. Therefore, it is adopted as the optimization tool in this study.

4.1.1 Algorithms

GA imitates the natural selection process of the population. It selects the fittest individuals to produce the offspring that fits the environment [32]. Generally, the algorithm considers five phases, namely initial population, fitness function, selection, crossover, and mutation.

The GA process starts with individuals known as a Population. Each individual is a potential solution to the problem to be solved. The characteristics of an individual correspond to a set of variables called Genes. A Chromosome is a string connected by Genes. In GA, a string of binary values (0 and 1) is generally applied to represent the set of genes. This research sets the best layout as the objective function, where the variables are coordinates and heights of all wind turbines. Figure 17 shows the chromosome and gene of the GA in this study.

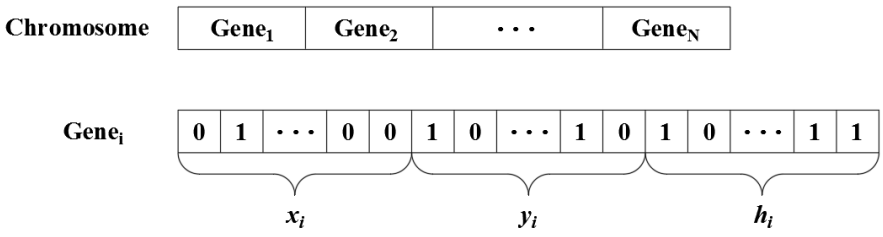

Figure 17 Chromosome and gene.

The spatial layout could be expressed by the positions and heights of turbines. Therefore, for a wind farm with N wind turbines, each chromosome has N genes, and each gene has three variables of x coordinate, y coordinate and hub height h. In this paper, the number of wind turbines in all cases is 30. To be started, the first population is randomly generated. Then, the fittest individuals are selected from the population. Their offspring reserves the characteristics of parents and add them to the next generation. If the fitness of parents is good, the offspring

can be better than their parents and have more chance of survival. This process keeps on iterating, and a generation with the fittest individuals can be obtained at the end.

4.1.2 Optimization framework – Problem formulation & Constraints

The spatial layout can be specified by the locations and heights of turbines, namely $X=[x_1,x_2,\cdots x_N]$, $Y=[y_1,y_2,\cdots y_N]$, and $H=[h_1,h_2,\cdots h_N]$. A general layout optimization problem is formulated as equation (6).

$$\left.\begin{array}{rll} \min & F_m(X,Y,H), & m=1,2,\cdots,M, \\ \text{subject to:} & G_k(X,Y), & k=1,2,\cdots,K; \\ & X^{(L)} \le X \le X^{(U)}; & \\ & Y^{(L)} \le Y \le Y^{(U)}; & \\ & H^{(L)} \le H \le H^{(U)}; & \end{array}\right\} \tag{6}$$

where F_m is the m^{th} objective function; G_k is the k^{th} constraint function; $X^{(L)}$, $X^{(U)}$, $Y^{(L)}$, $Y^{(U)}$, $H^{(L)}$, and $H^{(U)}$ are the lower and upper bounds.

F_m should be defined according to the problem at hand. Obtaining the maximum energy output and the minimum capital cost are two common objectives, which will be discussed in this study later.

G_k are subject to different constrains regarding to different consideration [33]. In this study, a constrain is involved into the consideration. To be specific, G_k represents that the minimal interval among wind turbines is 5D. The feasible area of all turbines is a square area of 2 km $\times$ 2 km, and the hub height ranges from 45 m to 85 m. Therefore, the boundary constrain is set as $X^{(L)}=0$, $X^{(U)}=2000$, $Y^{(L)}=0$, $Y^{(U)}=2000$, $H^{(L)}=45$, and $H^{(U)}=85$.

4.2 Case study

The information on wind turbine and incoming wind condition is presented in Section 2.2. The incoming wind is from north. The influence of hub height on wind farm is discussed from energy and economic aspects. All optimization work is completed using MTALAB software.

4.2.1 Energy as the optimization objective

In this part, obtaining wind farm's most power generation is set as the objective. Four different situations are studied, including the aligned layout with unit hub height, the aligned layout with optimized hub heights, the optimized layout with unit hub height, and the optimized layout and optimized hub heights.

1). Case E1 - Aligned layout-unit height

The wind farm is a 2 km × 2 km square area. In the aligned layout, positions of wind

turbines are fixed, which are shaped as 5 rows × 6 columns. The hub height of all wind turbines is set as 65 m. Figure 18 demonstrates the height and power of each wind turbine.

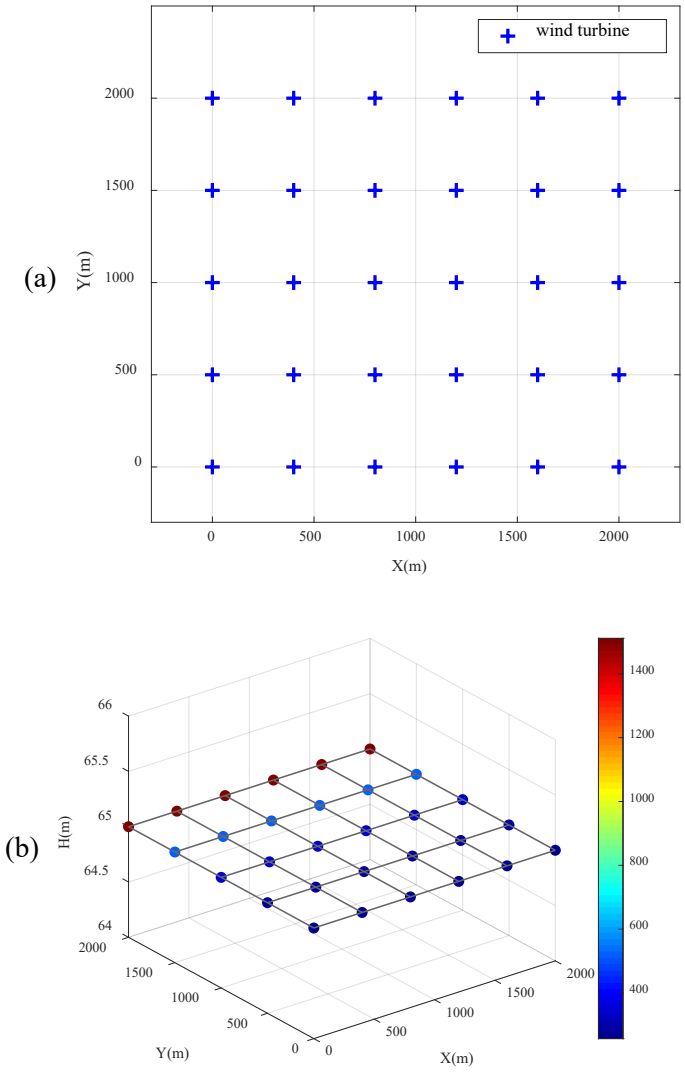

Figure 18 Result of Case E1: (a) Layout; (b) Hub height and power output.

In this case, there is no variable to be optimized. The result can be regarded as the benchmark. From Figure 18, the wake effect has significant impact on wind turbines. The first-row wind turbines reach 1513 kW, which is the rated power. The second-row turbine's power has a reduction to around 500 kW. The power continues to decrease in the downstream direction. The last turbine's power is approximately 300 kW. The wake effect causes serious power loss of downstream wind turbines, therefore the layout should be designed to reduce the wake influence.

2). Case E2 - Aligned layout-optimized height

This case study optimizes hub heights based on the previous aligned layout. Figure 19 demonstrates the height and power of each wind turbine.

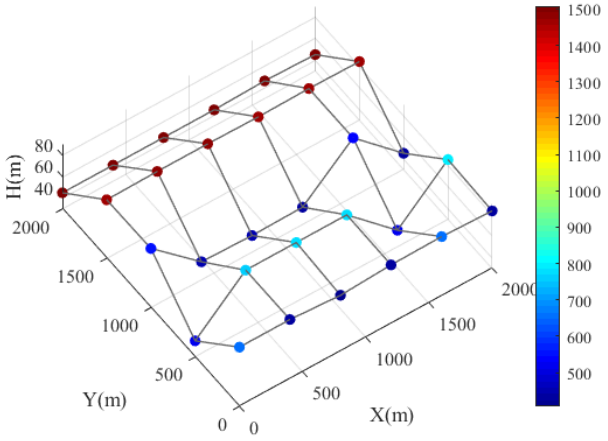

Figure 19 Result of Case E2: Hub height and power output.

As expected, the optimized hub heights are very different from the original 65 m hub height. The hub height between adjacent upwind and downwind turbines always has a huge difference. The optimized hub height in the first row is 45 m, and that in the second row is the upper limitation of 85 m. The power outputs of wind turbines increase significantly. From Figure 19, more wind turbines reach the rated power, and the minimum power output is larger than 400 kW. Actually, changing hub heights is changing the vertical relative positions between rotors, and the serious wake-influenced area can be avoided. Therefore, hub height optimization improves the power output of wind farm effectively.

3). Case E3 - Scattered layout-unit height

This case study optimizes the layout of wind turbines, and all hub heights are 65 m. Figure 20 shows the optimized layout and hub heights.

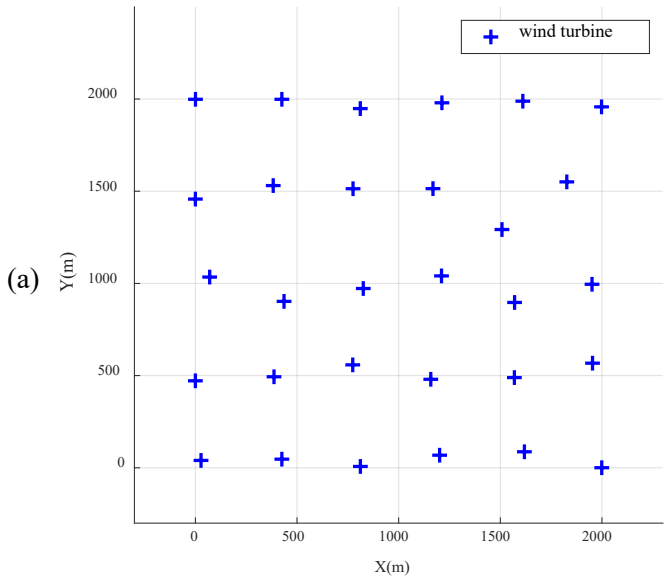

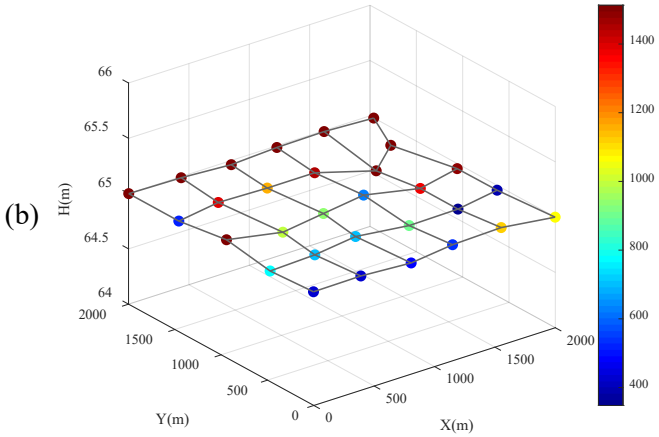

Figure 20 Result of Case E3: (a) Layout; (b) Hub height and power output.

Comparing with Case E1, optimizing wind farm's layout can also improve its power generation. The first-row wind turbines maintain the rated power, but all other wind turbines improve their power output by adjusting their positions. This method is a traditional idea to reduce the influence of wakes. By optimizing the layout, the horizontal relative positions between rotors changes to avoid the wake influence, which makes the wind farm to a better power performance.

4). Case E4 - Scattered layout-optimized height

This case study simultaneously optimizes the layout and hub heights of wind turbines. It takes 838 generations to obtain the optimized layout. The original expected computation time is more than 114 hours, while the actual computation time is only 20.1 hours. About 94 hours is saved during the complete process. Figure 21 demonstrates the results of Case E4.

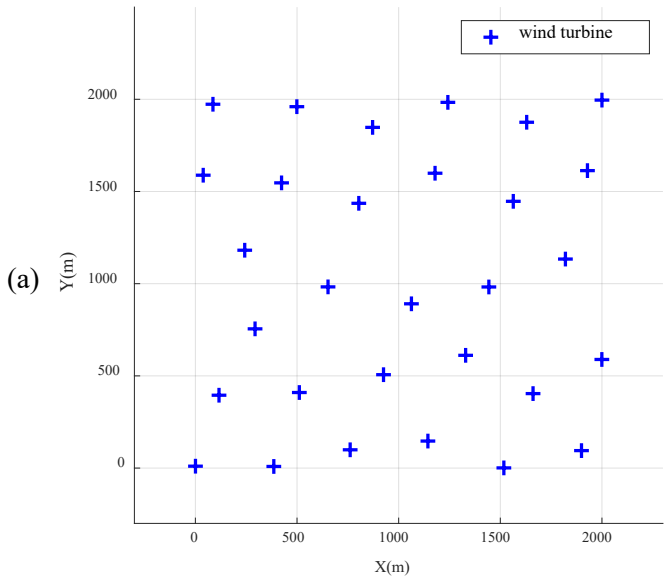

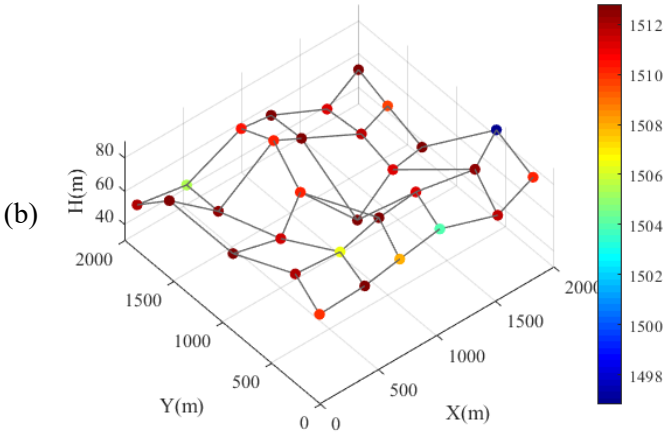

Figure 21 Result of Case E4: (a) Layout; (b) Hub height and power output.

The optimized hub heights tend to be small for front wind turbines, then increase in the downwind direction. Power output has an obvious improvement compared to results of previous cases. Since both layout and hub height can be changed individually to increase the power output of the wind farm, better results can be achieved by optimizing these two factors at the same time.

5). Summary

Table 3 compares the results of different cases. In all cases, the maximum power is the rated power of 1513kW. The mean powers and the minimum powers are very different, which results in a significant difference in the total power of each case. In Case E1, all hub heights are 65 m, and total power is only 17552 kW. By optimizing hub heights, the maximum height and the minimum height both reach the upper and lower limitations of 45 m and 85 m. The total power increases 58.9% to 27870 kW, indicating the good effectiveness of the hub height optimization. Comparing Case E3 and Case E1, optimizing the layout can increase 79.0% of the power output to 31418 kW, which is even more than 27870 kW in Case E2. If the layout and hub heights are optimized simultaneously, Case E4 can increase 158.1% of the total power to 45313 kW. The minimum power (1497 kW) is close to the mean power (1510 kW) and the maximum power (1513 kW), indicating that almost all wind turbines have reached their potential.

Table 3 Comparison of different cases.

Case	Case E1	Case E2	Case E3	Case E4
Maximum Power (kW)	1511	1507	1513	1513
Mean Power (kW)	585	929	1047	1510
Minimum Power (kW)	260	407	348	1497
Total Power (kW)	17552	27870	31418	45313

Maximum Height (m)	65	85	65	85
Mean Height (m)	65	68.9	65	68.8
Minimum Height (m)	65	45	65	45
Cost (USD)	4.57×10^7	4.71×10^7	4.57×10^7	4.68×10^7
Cost of Power (USD/kW)	2603	1689	1454	1033

4.2.2 Cost as the optimization objective

In the second part, the cost per kW energy is set as the optimization objective. As it is known to all, a higher hub height will lead to an increase in the capital cost. Therefore, a more comprehensive analysis involving the capital cost should be conducted. In this section, the evaluation criterion is defined as Cost of Power, which is the total power divided by total cost. Figure 22 demonstrates the estimation of total installed capital cost by the turbine and hub height.

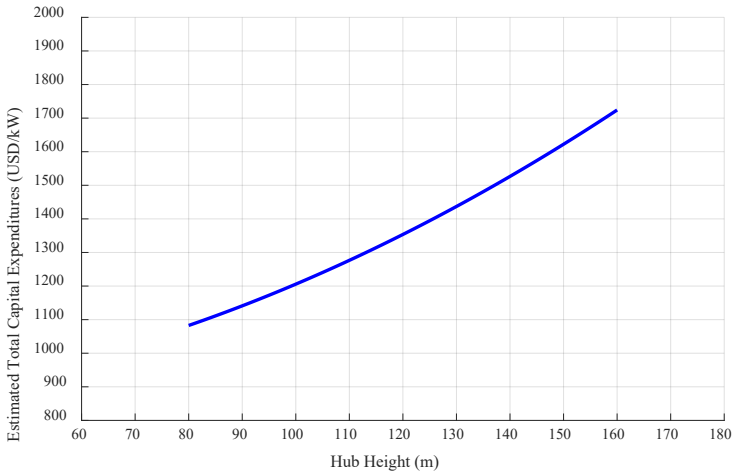

Figure 22 Estimated total installed capital cost by turbine and hub height [34].

1). Case C1 - Aligned layout-unit height

In Case C1, the layout and the hub height are fixed. Therefore, the strategy is the same as Case E1, and will not be discussed here.

2). Case C2 - Aligned layout-optimized height

This case study optimizes wind turbines' hub heights based on the aligned layout. Figure 23 demonstrates the height and power of each wind turbine.

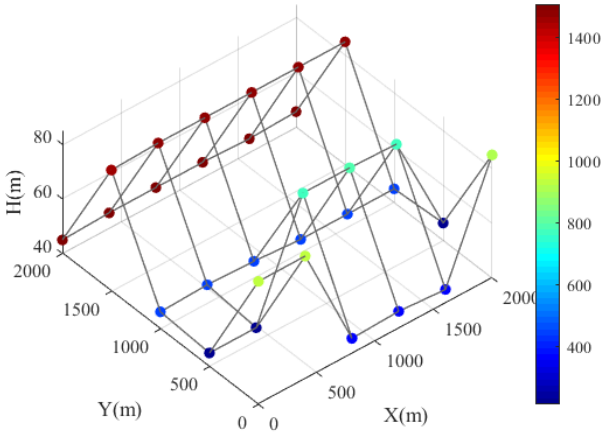

Figure 23 Result of Case C2: Hub height and power output.

The optimized height result has a similar pattern to Case E2. In the incoming wind direction, the adjacent turbines tend to have a huge height difference. However, since the cost is considered, there are fewer high wind turbines in this case than Case E2. High wind turbines may capture more wind energy and avoid wake influence, but the capital cost also increases with height. So, it is also important to estimate the cost factors when designing the layouts.

3). Case C3 - Scattered layout-unit height

In Case C3, since the hub height is fixed, the capital cost will not change. The objective of minimizing Cost of Power means maximizing the power output. Therefore, the optimization process is the same as Case E3, and the result of Case E3 is adopted in this case.

4). Case C4 - Scattered layout-optimized height

This case study simultaneously optimizes the layout and hub heights of turbines under the objective of minimizing COE. It takes 1017 generations to obtain the optimized layout. The original expected computation time is more than 138 hours, while the actual computation time is only 24.4 hours. About 113 hours is saved during the complete process. Figure 24 demonstrates the results of Case C4.

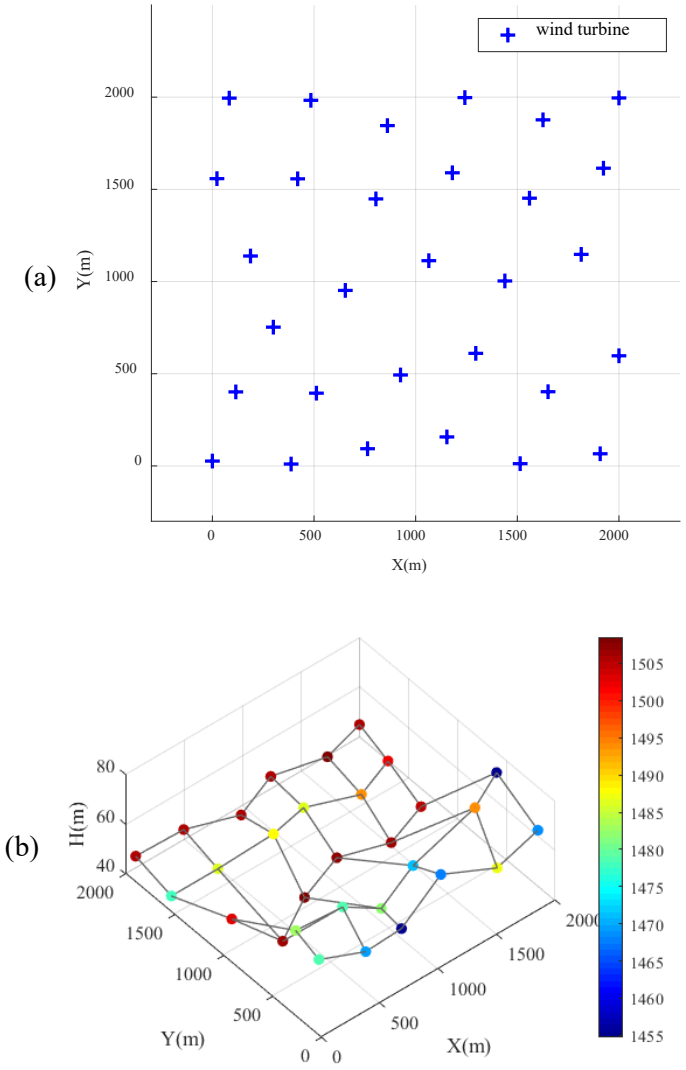

Figure 24 Result of Case C4: (a) Layout; (b) Hub height and power output.

The optimized layout pattern is scattered. Most hub heights are smaller than 65 m. Compared with results of other cases, power of each turbine is distributed more evenly. Similar to Case C2, cost has the inevitable impact on the results. This case study considers factors of layout, hub height and cost simultaneously, of which the results are the closest to actual engineering in all cases.

5). Summary

Table 4 compares results of cases in this section. As explained previously, Case C1 and Case C3 are the same as Case E1 and Case E3, respectively. Therefore, results of these two cases are also the same as previous two cases. Though cost is the optimization objective, the total power is also significantly improved. Compared with Case 1, the other three Cases C2, C3 and C4 increases the total power by 55.8%, 79.0% and 154.6%, respectively.

Compared with Case E2, the total power of Case C2 is smaller. The mean height of 61.3

m is smaller than that of Case E2, which is the main reason for the smaller power output. The hub heights of Case C4 are even smaller, with a maximum height of 74 m, a mean height of 53 m, and a minimum height of 45 m. Correspondingly, the total power is 44694 kW, which is also less than that of Case E4.

Table 4 Comparison of different cases.

Case	Case C1	Case C2	Case C3	Case C4
Maximum Power (kW)	1511	1508	1513	1509
Mean Power (kW)	585	912	1047	1490
Minimum Power (kW)	260	213	348	1455
Total Power (kW)	17552	27350	31418	44694
Maximum Height (m)	65	85	65	74
Mean Height (m)	65	61.3	65	53
Minimum Height (m)	65	45	65	45
Cost (USD)	4.57×10^7	4.55×10^7	4.57×10^7	4.36×10^7
Cost of Power (USD/kW)	2603	1662	1454	976

Table 5 compares the cost and Cost of Power of each case. Comparing Cases E2 and C2, Case E2 has more power output, but Case C2 has a lower Cost of Power. Therefore, increasing hub height can improve the power output, but it may not be the most economical method for designing a wind farm. The same phenomenon can be found in Cases E4 and C4. Case E4 has the maximum power output of all cases, while Case C4 has the minimum Cost of Power.

Table 5 Comparison of cost and COE

Case	Case E1	Case E2	Case E3	Case E4
Cost (USD)	4.57×10^7	4.71×10^7	4.57×10^7	4.68×10^7
Cost of Power (USD/kW)	2603	1689	1454	1033
Case	Case C1	Case C2	Case C3	Case C4
Cost (USD)	4.57×10^7	4.55×10^7	4.57×10^7	4.36×10^7
Cost of Power (USD/kW)	2603	1662	1454	976

The layout and hub height are two important factors that should be designed carefully when designing wind farms. Separately optimizing the layout and hub heights can both increase power generation of a wind farm. But simultaneously optimizing these two factors could obtain better results. Power output is a main parameter of concern for wind farms. However, the design with best power performance may not have the best economic performance. When determining a wind farm's hub heights, it is strongly recommended to account the capital together with the

power output.

5. Conclusions

This paper investigates the influence of hub height and layout optimization on power output of wind farm. Detailed conclusions are summarized as follows.

An engineering three-dimensional (3-D) wake model is introduced. To reduce the computational cost, Artificial neural network (ANN) is applied to improve the wake model, and a new 3-D ANN wake model is developed. The new model has a high accuracy of more than 99% of the original one. It can predict the wind speed at any spatial position quickly, and can save about 80% of computational time. This model is then adopted to optimize positions and hub heights of wind turbines.

Both hub heights and layout have prominent impact on equivalent wind speed (EWS) and power generation of wind turbines. For a single wind turbine, increasing hub height will increase EWS and power output, while decreasing the hub height has the opposite trend. The reason for this is the increasing trend of wind speed in the vertical direction. For two wind turbines, increasing the downwind and cross-wind intervals can both increase its EWS and power output. The influence of wake decreases with the increasing distance from the upstream wind turbine. On the other hand, the wake effect is most severe in the centerline region, thus changing the cross-wind spacing to avoid the wake's impact is another way to improve the efficiency of downstream wind turbines.

Special attention should be paid when changing the hub height of wind turbine. Increasing the hub height is beneficial to power output but decreasing it may have different results. The reason is that the negative influence of wakes decreases with the decreasing height, but the EWS will become smaller as well. The overall influence should be evaluated according to the specific changes in hub height and relative downstream distance.

The 3-D ANN wake model and the aforementioned findings have been applied to solve the wind farm layout and hub height optimization problems. Optimizing hub height or layout alone can increase the total power by more than 55% and 79%, while simultaneously optimizing these two factors can increase by 154%. The optimization result is significantly influenced by the objective. When power output is the only objective, the optimized hub heights tend to approach the upper height limitation. But if the economic factor is considered, the cost increases with the increasing height, so the optimized hub height may not be very high, and the power output does not reach the maximum as well. Therefore, how to balance cost and energy factors is a key point to designing the spatial layout of wind farm.

Acknowledgement

The work described in this paper was supported by *the Fundamental Research Funds for the Central Universities* with account number of D2220740, *National Natural Science Foundation of China* with account number of 52206248, *the Research Institute for Sustainable Urban Development (RISUD)* with account number of BBW8 and other Research projects with account numbers of ZVHL/BBAV, The Hong Kong Polytechnic University.

References

[1] S. Mathew, *Wind energy : fundamentals, resource analysis and economics*. Berlin: Springer, 2006.

[2] A. Altan, S. Karasu, and E. Zio, "A new hybrid model for wind speed forecasting combining long short-term memory neural network, decomposition methods and grey wolf optimizer," *Applied Soft Computing,* vol. 100, p. 106996, 2021/03/01/ 2021, doi: https://doi.org/10.1016/j.asoc.2020.106996.

[3] M. M. Alam, S. Rehman, J. P. Meyer, and L. M. Al-Hadhrami, "Review of 600–2500kW sized wind turbines and optimization of hub height for maximum wind energy yield realization," *Renewable and Sustainable Energy Reviews,* vol. 15, no. 8, pp. 3839-3849, 2011/10/01/ 2011, doi: https://doi.org/10.1016/j.rser.2011.07.004.

[4] M. Albadi and E. El-Saadany, "Optimum turbine-site matching," *Energy,* vol. 35, no. 9, pp. 3593-3602, 2010.

[5] K. Chen, M. X. Song, and X. Zhang, "The iteration method for tower height matching in wind farm design," *Journal of Wind Engineering and Industrial Aerodynamics,* vol. 132, pp. 37-48, 2014/09/01/ 2014, doi: https://doi.org/10.1016/j.jweia.2014.06.017.

[6] K. Chen, M. X. Song, and X. Zhang, "The investigation of tower height matching optimization for wind turbine positioning in the wind farm," *Journal of Wind Engineering and Industrial Aerodynamics,* vol. 114, pp. 83-95, 3// 2013, doi: http://dx.doi.org/10.1016/j.jweia.2012.12.010.

[7] K. Chen, M. X. Song, X. Zhang, and S. F. Wang, "Wind turbine layout optimization with multiple hub height wind turbines using greedy algorithm," *Renewable Energy,* vol. 96, pp. 676-686, 2016/10/01/ 2016, doi: https://doi.org/10.1016/j.renene.2016.05.018.

[8] Y. Chen, H. Li, K. Jin, and Q. Song, "Wind farm layout optimization using genetic algorithm with different hub height wind turbines," *Energy Conversion and Management,* vol. 70, pp. 56-65, 2013/06/01/ 2013, doi: https://doi.org/10.1016/j.enconman.2013.02.007.

[9] J. Lee, D. R. Kim, and K.-S. Lee, "Optimum hub height of a wind turbine for maximizing annual net profit," *Energy Conversion and Management,* vol. 100, pp. 90-96, 2015/08/01/ 2015, doi: https://doi.org/10.1016/j.enconman.2015.04.059.

[10] S. A. MirHassani and A. Yarahmadi, "Wind farm layout optimization under uncertainty," *Renewable Energy,* vol. 107, pp. 288-297, 2017/07/01/ 2017, doi: https://doi.org/10.1016/j.renene.2017.01.063.

[11] M. Abdulrahman and D. Wood, "Investigating the Power-COE trade-off for wind farm layout optimization considering commercial turbine selection and hub height variation," *Renewable Energy,* vol. 102, Part B, pp. 267-278, 3// 2017, doi: http://dx.doi.org/10.1016/j.renene.2016.10.038.

[12] A. Vasel-Be-Hagh and C. L. Archer, "Wind farm hub height optimization," *Applied Energy,* vol. 195, pp. 905-921, 2017/06/01/ 2017, doi: https://doi.org/10.1016/j.apenergy.2017.03.089.

[13] P. P. Biswas, P. N. Suganthan, and G. A. J. Amaratunga, "Decomposition based multi-objective evolutionary algorithm for windfarm layout optimization," *Renewable Energy,* vol. 115, pp. 326-337, 1// 2018, doi: https://doi.org/10.1016/j.renene.2017.08.041.

[14] M. Song, K. Chen, and J. Wang, "Three-dimensional wind turbine positioning using Gaussian particle swarm optimization with differential evolution," *Journal of Wind Engineering and Industrial Aerodynamics,* vol. 172, pp. 317-324, 1// 2018, doi: https://doi.org/10.1016/j.jweia.2017.10.032.

[15] H. Sun and H. Yang, "Study on an innovative three-dimensional wind turbine wake model," *Applied Energy,* vol. 226, pp. 483-493, 2018/09/15/ 2018, doi: https://doi.org/10.1016/j.apenergy.2018.06.027.

[16] B. Dou, T. Qu, L. Lei, and P. Zeng, "Optimization of wind turbine yaw angles in a wind farm using a three-dimensional yawed wake model," *Energy,* vol. 209, p. 118415, 2020/10/15/ 2020, doi: https://doi.org/10.1016/j.energy.2020.118415.

[17] X. Gao *et al.*, "Investigation and validation of 3D wake model for horizontal-axis wind turbines based on filed measurements," *Applied Energy,* vol. 260, p. 114272, 2020/02/15/ 2020, doi: https://doi.org/10.1016/j.apenergy.2019.114272.

[18] Z. Ti, X. W. Deng, and H. Yang, "Wake modeling of wind turbines using machine learning," *Applied Energy,* vol. 257, p. 114025, 2020/01/01/ 2020, doi: https://doi.org/10.1016/j.apenergy.2019.114025.

[19] Z. Ti, X. W. Deng, and M. Zhang, "Artificial Neural Networks based wake model for power prediction of wind farm," *Renewable Energy,* vol. 172, pp. 618-631, 2021/07/01/ 2021, doi: https://doi.org/10.1016/j.renene.2021.03.030.

[20] Z. Luo, W. Luo, J. Xie, J. Xu, and L. Wang, "A new three-dimensional wake model for the real wind farm layout optimization," vol. 40, no. 2, pp. 701-723, 2022, doi: 10.1177/01445987211056989.

[21] Z. Zhen, W. Zhao, and S. Li, "Wind farm layout optimization based on 3D wake model and surrogate model," *International Journal of Green Energy,* pp. 1-11, 2021, doi: 10.1080/15435075.2021.1976651.

[22] N. O. Jensen, *A note on wind generator interaction*. 1983.

[23] W. Schlez, A. Tindal, and D. Quarton, "GH wind farmer validation report," Garrad Hassan and Partners Ltd, Bristol,, 2003.

[24] Y.-T. Wu and F. Porté-Agel, "Large-eddy simulation of wind-turbine wakes: evaluation of turbine parametrisations," *Boundary-layer meteorology,* vol. 138, no. 3, pp. 345-366, 2011.

[25] E. Djerf and H. Mattsson, "Evaluation of the software program windfarm and comparisons with measured data from alsvik," *The aeronautical research institute of Sweden,* 2000.

[26] H. Sun and H. Yang, "Numerical investigation of the average wind speed of a single wind turbine and development of a novel three-dimensional multiple wind turbine wake model," *Renewable Energy,* vol. 147, pp. 192-203, 2020/03/01/ 2020, doi: https://doi.org/10.1016/j.renene.2019.08.122.

[27] H. Sun, X. Gao, and H. Yang, "Experimental study on wind speeds in a complex-terrain wind farm and analysis of wake effects," *Applied Energy,* vol. 272, p. 115215, 2020/08/15/ 2020, doi: https://doi.org/10.1016/j.apenergy.2020.115215.

[28] X. Gao *et al.*, "Investigation of wind turbine performance coupling wake and topography effects based on LiDAR measurements and SCADA data," *Applied Energy,* vol. 255, p. 113816, 2019/12/01/ 2019, doi: https://doi.org/10.1016/j.apenergy.2019.113816.

[29] J. F. Manwell, J. G. McGowan, and A. L. Rogers, *Wind energy explained: theory, design and application*. John Wiley & Sons, 2010.

[30] H. Sun, X. Gao, and H. Yang, "Validations of three-dimensional wake models with the wind field measurements in complex terrain," *Energy,* vol. 189, p. 116213, 2019/12/15/ 2019, doi: https://doi.org/10.1016/j.energy.2019.116213.

[31] H. Sun, H. Yang, and X. Gao, "Investigation into spacing restriction and layout optimization of wind farm with multiple types of wind turbines," *Energy,* vol. 168, pp. 637-650, 2019/02/01/ 2019, doi: https://doi.org/10.1016/j.energy.2018.11.073.

[32] X. Ju, F. Liu, L. Wang, and W.-J. Lee, "Wind farm layout optimization based on support vector regression guided genetic algorithm with consideration of participation among landowners," *Energy Conversion and Management,* vol. 196, pp. 1267-1281, 2019/09/15/ 2019, doi: https://doi.org/10.1016/j.enconman.2019.06.082.

[33] J. Feng, W. Z. Shen, and Y. Li, "An Optimization Framework for Wind Farm Design in Complex Terrain," *Applied Sciences-Basel,* vol. 8, no. 11, Nov 2018, Art no. 2053, doi: 10.3390/app8112053.

[34] E. Lantz, O. Roberts, J. Nunemaker, E. DeMeo, K. Dykes, and G. Scott, "Increasing Wind Turbine Tower Heights: Opportunities and Challenges," National Renewable Energy Laboratory, 2019. [Online]. Available: https://www.nrel.gov/docs/fy19osti/73629.pdf